RECOVERY OF ZnO FROM LEAD-ZINC FLOTATION TAILINGS BY HYDROMETALLURGICAL PROCESSES – XRD, SEM, AND AFM STUDIES

K.T. Perek[1], B. Benli[1], C. Arslan[2], F. Arslan[1]#

[1]Istanbul Technical University, Mineral Processing Engineering Department, Istanbul, Turkey
[2]Istanbul Technical University, Metallurgical and Material Engineering Department, Istanbul, Turkey

Abstract

The hydrometallurgical route of zinc hydroxide and synthesis of nanocrystalline ZnO is a particularly attractive method to recover oxidized lead and zinc from lead-zinc flotation tailings. In Turkey, lead-zinc complex/mixed ores along with high iron content are not suitable for conventional mineral processing methods and need hydrometallurgical treatments. Therefore, the control of iron during zinc processes is really important. In this study, hydrometallurgical process route for zinc recovery from Pb-Zn flotation tailings was investigated by considering the effects of H_2SO_4 concentration, leaching and roasting temperatures on the zinc dissolution considering the Eh-pH variations. The iron and zinc products were also individually examined by X-ray Diffraction (XRD), Scanning Electron Microscopy (SEM) and Atomic Force Microscopy (AFM) images in order to compare before and after leaching, precipitation and roasting steps. 83.1% Zn and 91.6% Cd leaching efficiencies were obtained from Pb-Zn flotation tailing particles with the size range of 50-110 nm from AFM image cross-sections, while lead and iron were not dissolved. Elemental sulfur started to form and produce a layer around the particles or a partially agglomerated particle in the size of 170 nm during the sulphuric acid leaching. However, majority of the particles was determined to be less than 20 microns, and AFM images showed that the size reduction between the leached and unleached particles was over 50%.

Selective precipitations of iron and zinc in the form of hydroxide were performed in high recovery efficiencies of 90.1% and 99%, respectively. After the heat treatment, nanocrystalline zincite clusters of 96.6% purity were produced in the ZnO mineral form and nearly 13 nm in size. Zinc can be successfully recovered and a flotation tailings ore can be a good candidate for the production of high technology needs of nanocrystalline ZnO nanoparticles.

Key words: Pb-Zn ores; Leaching; Precipitation; Zinc oxide clusters; Zincite structure.

1. Introduction

Zinc, especially in the form of zinc oxide (ZnO), is the key element for semiconductor and piezoelectric materials in electronics, optics, and photonics, as well as the raw material for other important industrial applications including white pigment, plastics, ceramics, glass, cement, paints, and fire retardants, etc. [1]. Since zinc oxide shows different purity and particle characteristics depending on the synthesis methods [2, 3], many grades of ZnO particles [4] could be synthesized to meet the diverse industry requirements such as controlled burning of zinc metal vapor in air (French process), chemical vapor deposition, electrodeposition, pulsed laser deposition, sol-gel synthesis, and spray pyrolysis. Among them, room temperature solution route (hydro-thermal method) is particularly attractive because it is a simple and catalyst-free process.

The hydrometallurgical route of zinc oxide is primarily based on zinc hydroxide or basic zinc carbonate [5, 6]. The common recovery method of oxidized lead and zinc minerals from lead-zinc ores at present is flotation in practice [7 - 9]. In Turkey, there are lead - zinc complex/mixed ores with high iron content that are not suitable for concentration with conventional mineral processing methods due to their complex mineralogy and need hydrometallurgical treatment [10, 11]. Even the most efficient concentrators generally produce zinc concentrate with significant iron content. Therefore, iron is usually removed from leaching solutions by precipitation methods such as jarosite, goethite, paragoethite, and hematite processes [12 - 16]. However,

some environmental problems become evident during the disposal of jarosite. In order to overcome these problems, it is required to remove iron from aqueous solutions as marketable iron products such as hematite which can be used as a pigment and a raw material in iron-steel industry. Besides, the world's zinc production is mostly obtained by the roast-leach-electrowinning processes. Since zinc electrowinning needs very pure zinc sulphate solution, the purification process is one of the most important downstream unit processes in zinc hydro/electrometallurgy. Zinc can be easily precipitated as hydroxide after iron removal from solution by simply adjusting the pH values.

The use of industrial residues or Pb-Zn ore flotation tailings [17, 18] appears attractive in order to improve innovative products through conventional technology and possibly a good candidate to improve resource management, energy efficiency and environmental impacts, i.e. recovery of metallic zinc from galvanizing plant wastes [19], recycling of ZnO flue dust [20], electric arc furnace dust [21], and scrapped lead acid batteries [22]. Recovery and recycling of valuable materials, in our case Zn-hydroxide recovery, from industrial residues also reduce the amount of wastes to be finally disposed and thus reduce the waste disposal problems. These days, environmental and economic considerations coupled with scientific and technological developments have again brought into focus the tailings ponds as potential sources of raw materials.

The aim of this experimental work was to make a consideration to improve the recovery of ZnO particles from the flotation tailings of the Lead-Zinc-Copper Concentration Plant. In this study, Scanning Electron Microscopy (SEM) and Atomic Force Microscopy (AFM) images of the Pb-Zn flotation tailings before and after the leaching and precipitation processes were used to understand how hydrometallurgical route affected the particle characteristics such as the shape and size of iron and zinc particles during ZnO production from Pb-Zn flotation tailings.

2.   Materials and methods

The dry fine flotation tailings used in this experimental study were obtained from a flotation plant of complex lead-zinc oxide ores (containing 10.17% Pb, 10.98% Zn, 57 g/t Ag, and 164 g/t Cd) located near Kayseri-Aladağ region of Turkey. The chemical analysis of the sample was carried out by XRF analyzer (Thermo Scientific NITON XL3t) and the Zn, Pb, and Fe content of

representative flotation tailings sample were found as 7.74%, 2.66%, and 21.24%, respectively.

Figure 1 shows the experimental flowsheet for both leaching and precipitation steps. First step was hot acid leaching experiments using sulfuric acid (Merck, 95-98% purity) to dissolve only Zn and Cd since Pb does not dissolve in H_2SO_4 solutions. Acidic leaching experiments were carried out in a 2-L beaker and continuously agitated by a mechanical stirrer at specified temperatures. The redox potential (Eh) and pH were also periodically measured. After filtered and washed with distilled water, the leach residues were separated. Leach liquors were analyzed for Zn, Cd, and Fe by Atomic Absorption Spectrometer (AAS) of Perkin-Elmer.

In the second step, selective precipitation of iron was carried out at pH 4 by chemical precipitation. Iron hydroxide was separated by filtration and the remaining solution was sent to zinc precipitation.
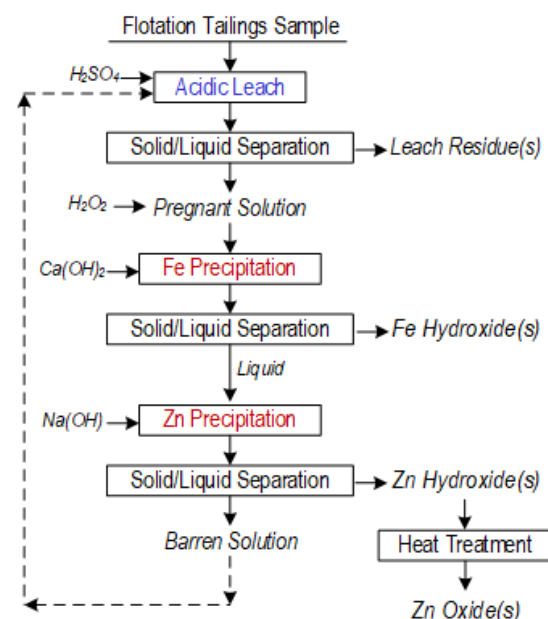
Figure 1 Experimental flowsheet for recovering ZnO from lead-zinc ore flotation tailings

In the third step, Zn-hydroxide was precipitated at 40°C and pH 11-12 using the same set-up of Fe-precipitation. After filtration, Zn-hydroxide precipitate was washed with distilled water several times and dried at 105°C. The dried Zn-hydroxide was then subjected to heat treatment to produce ZnO at 1100°C for 30 min. The phase composition of the prepared zinc oxide was determined by X-Ray Diffraction (XRD) analysis, Scanning

Electron Microscopy (SEM) and Atomic Force Microscopy (AFM) images as suggested in the literature [23].

Characterization studies conducted by using XRD, SEM and AFM are explained below:

X-Ray Diffraction (XRD) Analysis: The crystal structure of the precipitate was characterized by X-Ray Diffraction (XRD) analysis (BRUKER X-ray Diffractometer model 'Advanced D8') using CuK_{α} (λ=0.15418 nm) at 40 kV and 250 mA. Data was collected at room temperature at 2θ = 10° to 90°.

Scanning Electron Microscopy (SEM) Analysis: SEM images were obtained using a Hitachi S-3000H scanning electron microscope (Hitachi, Tokyo, Japan). Images were obtained from the leaching and precipitation media after leach and precipitation process for iron, zinc, and zinc oxide product. The SEM images of the samples were taken under the following conditions: 1024x1024 pixel; voltage, 15 kV; probe size, 20 nm; magnification, 5,000x.

Atomic Force Microscopy (AFM) Imaging and Size Measurement Procedure: The depositing procedure on high-quality mica was previously defined for sepiolite fibers [24], montmorillonite, and smectite type clay minerals [25, 26]. To spread precipitated Fe and Zn suspension (0.1 g in 50 ml H_2O), a dilute suspension of 1 ml was dropped on the freshly cleaved mica surface followed by drying the sample in a Petri dish at room conditions for 24 hours. Before taking images, samples were cleaned by blowing nitrogen gas through the substrate. The AFM measurements were obtained using Park System XE70 Atomic Force Microscopy (Park System, Park Systems Corp., Suwon, Korea). AFM-contact mode was performed using 910 M-NSC36/Cr–Au-type cantilevers with 0.5 Hz scanning speed and acquisition points were 515x512. The AFM tips were cleaned by a UV ozone cleaner chamber (UV/Ozone ProCleaner, Bioforce Nanosciences Inc., IA, US) under UV radiation for 30 min prior to use. In order to provide a three-dimensional surface profile and height measurements corresponds to the diameter or size of the particle with a high degree of accuracy and precision, AFM images of the samples such as tailings particles, leaching products, zinc oxide and iron precipitate particles were also processed by XEI software (Park Systems Corp., Suwon, Korea). There are also some characterization studies by AFM on ZnO particles and coatings [27 - 29].

3.   Results and discussion

Experimental results were discussed in two main parts namely hydrometallurgical processes (hot acidic leaching, iron precipitation, and zinc hydroxide precipitation) followed by the heat treatment, and studies on SEM and AFM images of all products.

3.1.   Hydrometallurgical Processes with Pb-Zn flotation tailings

3.1.1. Acidic leaching studies

In these tests the effect of acid concentration, temperature, and roasting prior to leaching on metal dissolution efficiencies was tested. Eh-pH measurements were also carried out.

Effect of acid concentration:
The constant experimental conditions were provided as 60°C temperature, 1/10 S/L ratio, 60 min of leaching time, and 400 rpm stirring speed where acid concentration varied between 0-80 g/L. Figure 2 shows the effect of acid concentration on the zinc dissolution where Figure 3 indicates the Eh-pH variations during leaching process further indicating the dissolution areas of Zn (Figure 4) and Fe (Figure 5). Zinc dissolution efficiency increased gradually up to 60 g/L acid (H_2SO_4) concentration and stabilized after that point. The highest Zn leaching efficiency was 90% at 80 g/L acid concentration with an acid consumption of 579 kg/t.
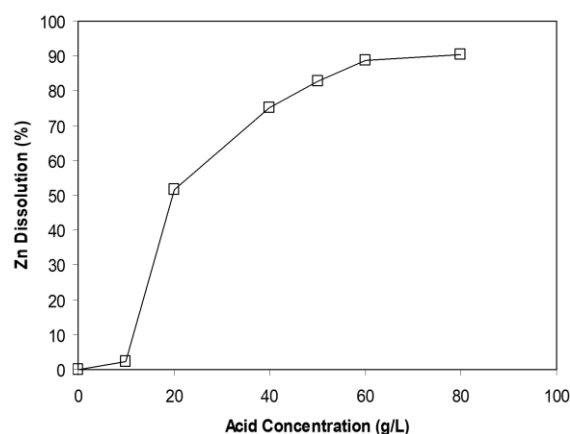
Figure 2 Effect of acid concentration on Zn dissolution efficiency
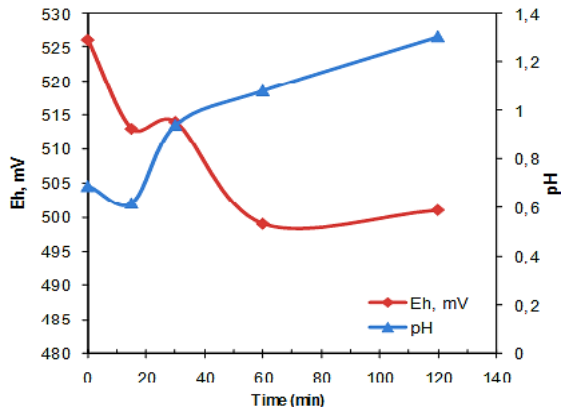
Figure 3 Eh (potential) and pH variations versus time during zinc leaching process
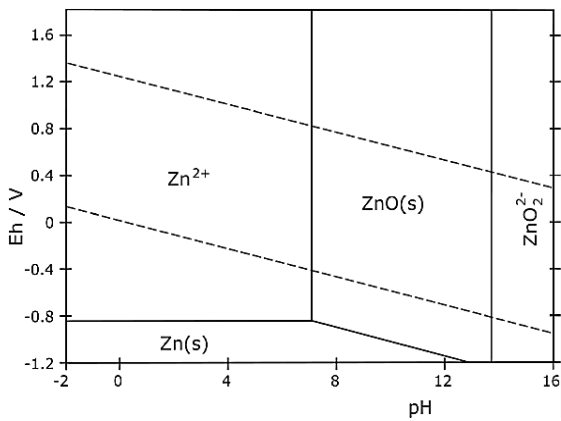
Figure 4 Eh and pH diagram for Zn-water system [30]
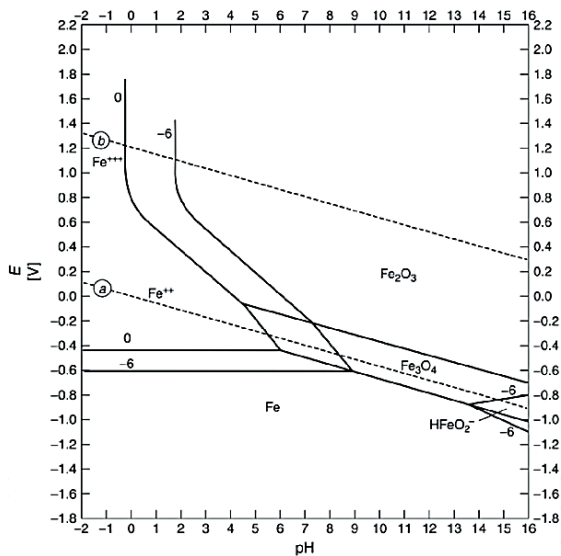
Figure 5 Eh and pH diagram for Fe-water system [30]

Effect of temperature:

Experiments were run under constant conditions of 60 g/L acid concentration, 1/10 S/L ratio, and 400 rpm stirring speed. The effect of temperature (between 20-80°C) on Zn dissolution relative to leaching time is shown in Figure 6. Increasing temperature increased the curves to the higher values up to 60°C temperature and no further increase was observed; therefore, 60°C was found as the optimum temperature for effective zinc dissolution and 30 min of leaching time was also sufficient.

The optimum leaching conditions were found as 30 min of leaching time, 60°C of leaching temperature and 60 g/L of acid concentration. 91.5% Zn, 79.2% Cd, and 14.3% Fe leaching efficiencies were obtained at the optimum conditions while Pb remained in the leaching residue, and the acid consumption was about 467 kg/t.
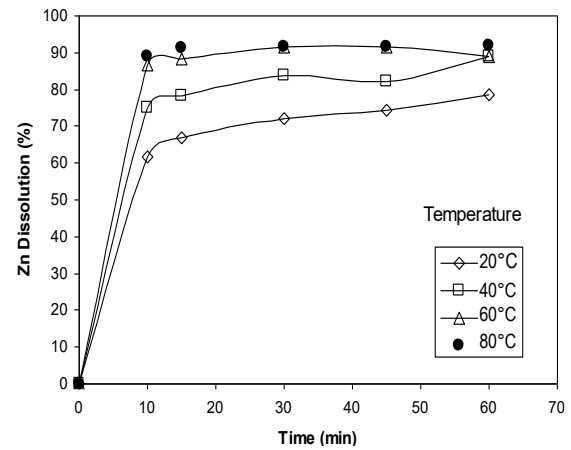
Figure 6 Effect of leaching temperature on Zn dissolution

Effect of roasting prior to leaching:

In the roasting-acidic leaching experiments, the effects of roasting temperature, leaching temperature, and acid concentration on the zinc dissolution efficiency of the calcine were investigated [31]. The constant experimental conditions of leaching were 20 g/L acid (H_2SO_4) concentration, 1/5 S/L ratio, 1 hour leaching time, and 400 rpm stirring speed. Figure 7 shows the effect of roasting temperature in relation to leaching temperature and as seen 400°C of roasting temperature and 60°C leaching temperature were found to be the optimum.

The optimum leaching conditions were 60°C leaching temperature, 1/5 S/L ratio, 1 hour leaching time, and 400 rpm stirring speed. Effect of acid concentration on Zn

dissolution from the calcine roasted at 400°C is shown in Figure 8. Increasing the acid concentration had an increasing effect up to 50 g/L acid concentration and did not change after that point. Therefore, 50 g/L acid concentration was found as the optimum value. On the other hand, using the optimum leaching conditions, 83.1% Zn and 91.6% Cd dissolution efficiencies were obtained while lead and iron were not dissolved and the acid consumption was around 442.9 kg/t.
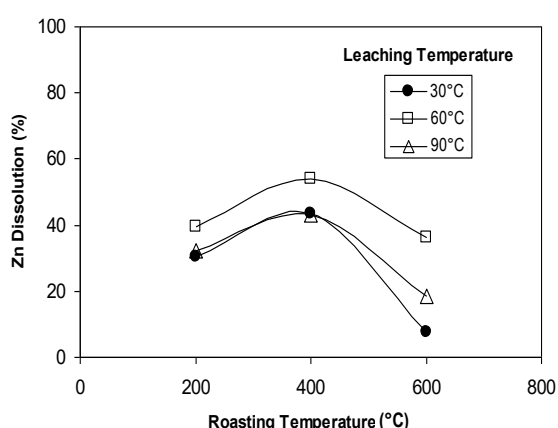
Figure 7 Effect of roasting and leaching temperatures on Zn dissolution
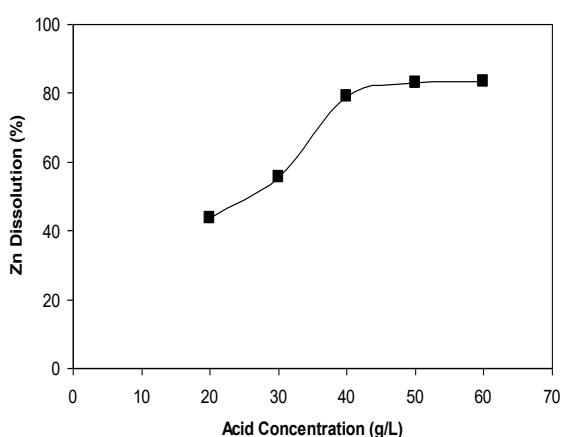
Figure 8 Effect of acid concentration on Zn dissolution from calcine

The leaching reaction of zinc oxide by sulfuric acid solutions can be expressed as follows:

$$ZnO+H_2SO_4 \rightarrow ZnSO_4+H_2O \tag{1}$$

Similar to this experimental study, Yoshida (2003) analyzed the effects of temperature, agitation speed,

initial acid concentration, and particle size on the kinetics of zinc extraction from EAF dusts in a sulfuric acid solution on the basis of above reaction [32]. The activation energy of the zinc oxide leaching with sulfuric acid was found 17.5 kJ/mol by the Arrhenius plot showing that the reaction rate of zinc oxide leaching was controlled by mass transfer through the liquid boundary layer. Activation energy was also calculated as 20.7 kJ/mol in the temperature range of 313 K to 353 K, for zinc recovery from metal oxide varistors (MOVs) with sulfuric acid [33].

3.1.2. Selective Precipitation of Iron and Zinc

Iron was precipitated from leach solutions at 60°C temperature and a pH range of 4.2-4.3 by adding $Ca(OH)_2$. Figure 9 gives the Eh-pH variation versus time during the selective iron precipitation experiments. Fe precipitation efficiency was about 90.1%. However, a small amount of Zn precipitation was also observed along with Fe. Then, zinc was precipitated in hydroxide form at 40°C and pH of 11-12 adjusted by the addition of NaOH according to the following reaction with 99% efficiency:

$$ZnSO_4+4NaOH \rightarrow Zn(OH)_2+H_2SO_4 \tag{2}$$
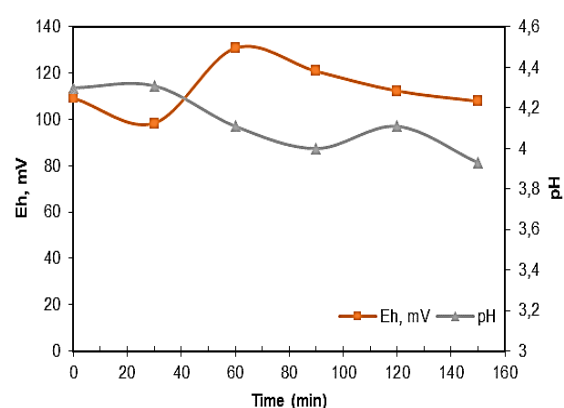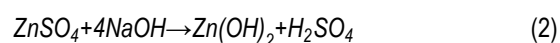
Figure 9 Eh-pH variation versus time during the precipitation of iron

3.1.3. Nanocrystalline ZnO powders production

Zinc hydroxide was subjected to heat treatment to produce ZnO at 1100°C according to the following reaction:

$$Zn(OH)_2 \rightarrow ZnO+H_2O \tag{3}$$

X-ray powder diffraction pattern of the ZnO precipitate can be seen in Figure 10. The XRD pattern of

ZnO phase was in agreement with synthetic zincite. The diffraction peaks in the pattern can be indexed to hexagonal zincite structure which is the mineral form of ZnO with no impurity of Zn and $Zn(OH)_2$. The purity of ZnO product as a result of the experimental procedure (Figure 1) was found at 96.6%.
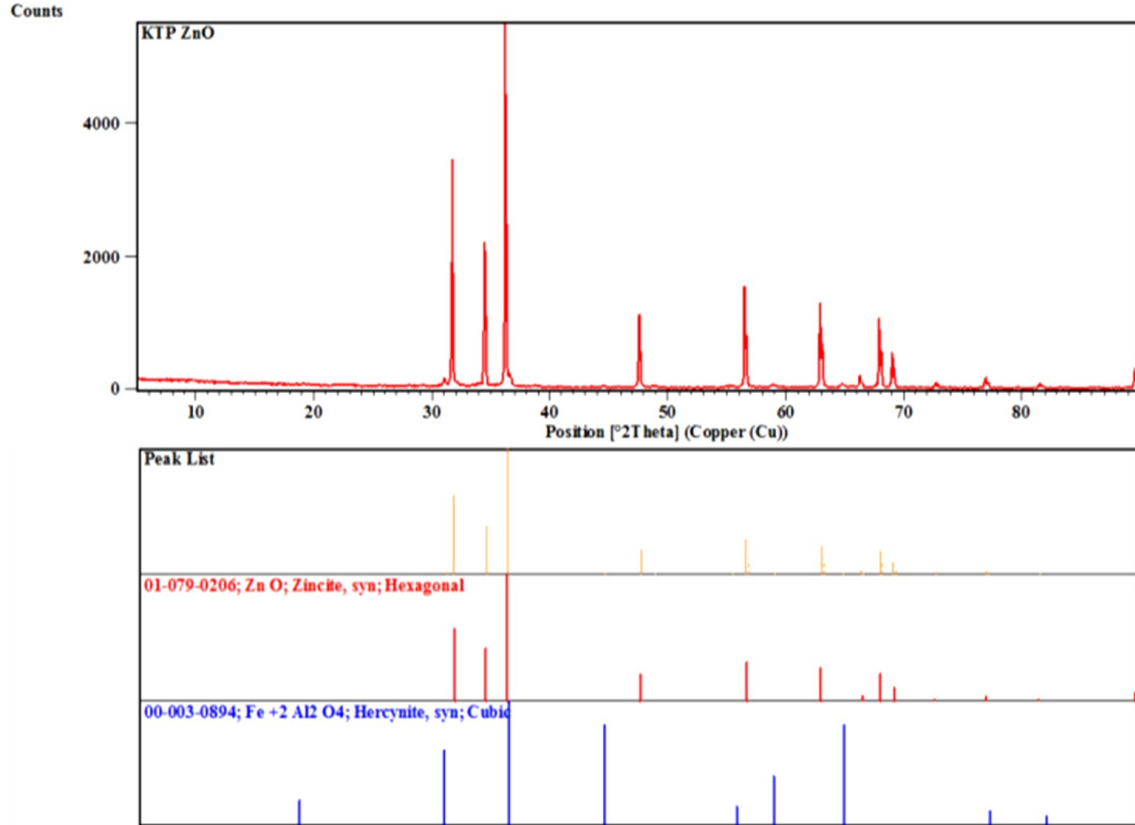
Figure 10 XRD analysis of ZnO

3.2. SEM and AFM Characterization of hydrometallurgical route products and zinc oxide

Figure 11 shows Atomic Force Microscopy (AFM) image of Pb-Zn flotation tailing particles with a clear surface. The flotation tailing sample included the larger and the smaller dispersed particles after stirring in water for 5 min. The sizes of these particles were measured from their three-dimensional surface profile (Figure 12). Although the lateral dimensions were influenced by the shape of the probe, the height measurements provided very useful information about the height of the tailing particles with a high degree of accuracy and precision. If the particles were assumed to be spherical, the height measurements corresponded to the diameters or sizes of the particles for the larger (red line) and smaller particles (green line) were determined approximately 110 nm and 50 nm, respectively.
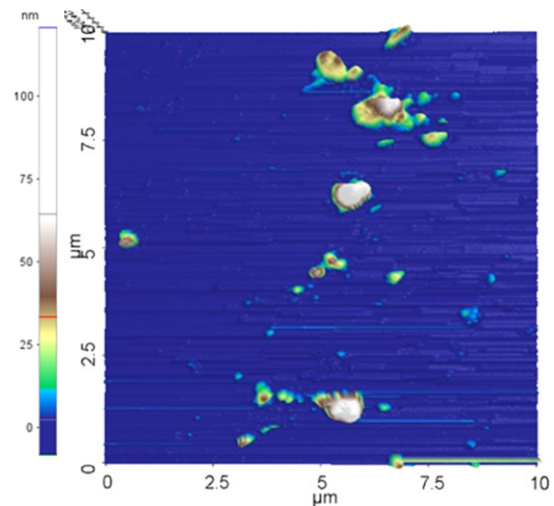
Figure 11 AFM image of dispersed particles taken from Pb-Zn flotation tailings
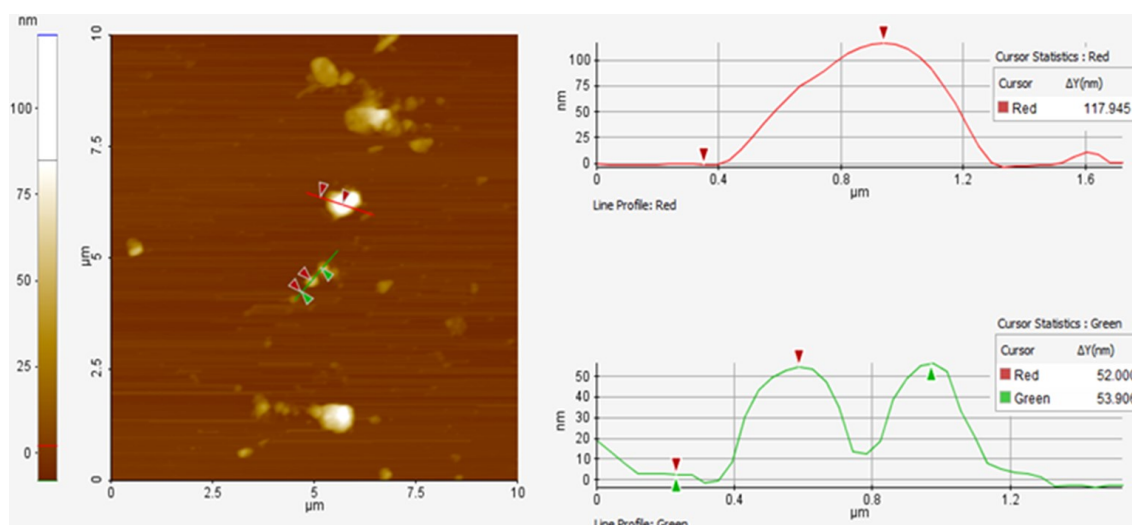
Figure 12 AFM image and cross-sections for 50 nm (green) and 100 nm (red) nanoparticles (nominal) deposited on a fresh mica substrate; the differences between the peak height and the average baseline correspond to the particle height of dispersed tailings particles after 5 min stirring in water

During the sulfuric acid leaching step, elemental sulfur started to form and produce a layer around the particles proven by XRD and SEM analysis before [31, 34]. Similar situations in accordance with previous studies were also observed in this study. Figure 13 shows the SEM image of the leach residue particles after 60 min of leaching at 60°C. The surface of leach residue obtained was probably covered by elemental sulfur, therefore this may be a reason of decreasing dissolution rate after 60 mins of leaching. Similarly, the AFM image of leach residues in Figure 14 suggests that particles varied in size and that there was an increase in the amount of fine particles. Further processing, the leach residue showed a large particle size distribution according to their three-dimensional surface profile (Figure 15). Large particles can be identified as partially agglomerated particles (Red line profiles) as 170 nm, 22 nm, and 19 nm of height distributions, whereas majority of the particles was determined to be less than 20 microns. To enhance the leaching efficiency in acidic sulfate solutions, silver, cupric and ferrous ions, and lignosol (sodium lignosulphonate) may be added [31, 34], mechanical activation/turbo-mill grinding may be helpful to crack the sulfur layer [35].

Leached particles with and without pre-roasted were deposited on a mica substrate, and then imaged by thr AFM contact mode (Fig. 16). The roasted tailings prior to leaching and its effect on the sizes of precipitated Fe particles were investigated from the cross-sectional profiles of the images (Fig. 17).
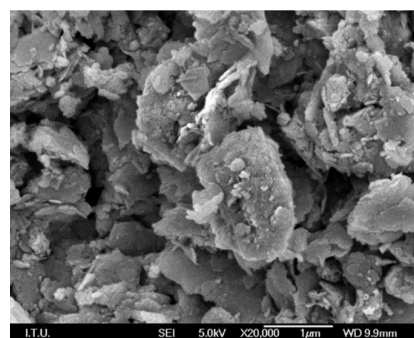
Figure 13 SEM photograph of leach residue
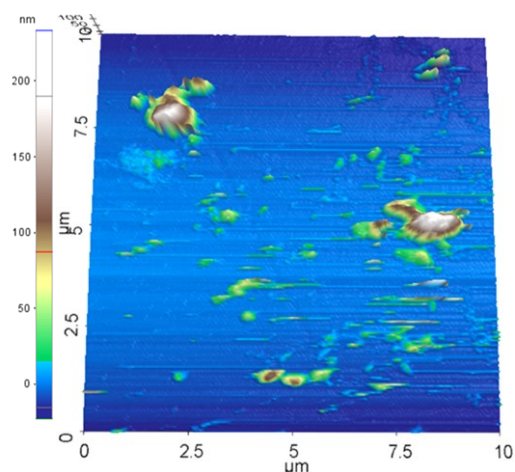
Figure 14 AFM image of dispersed particles from leach residue after 5 min stirring in water
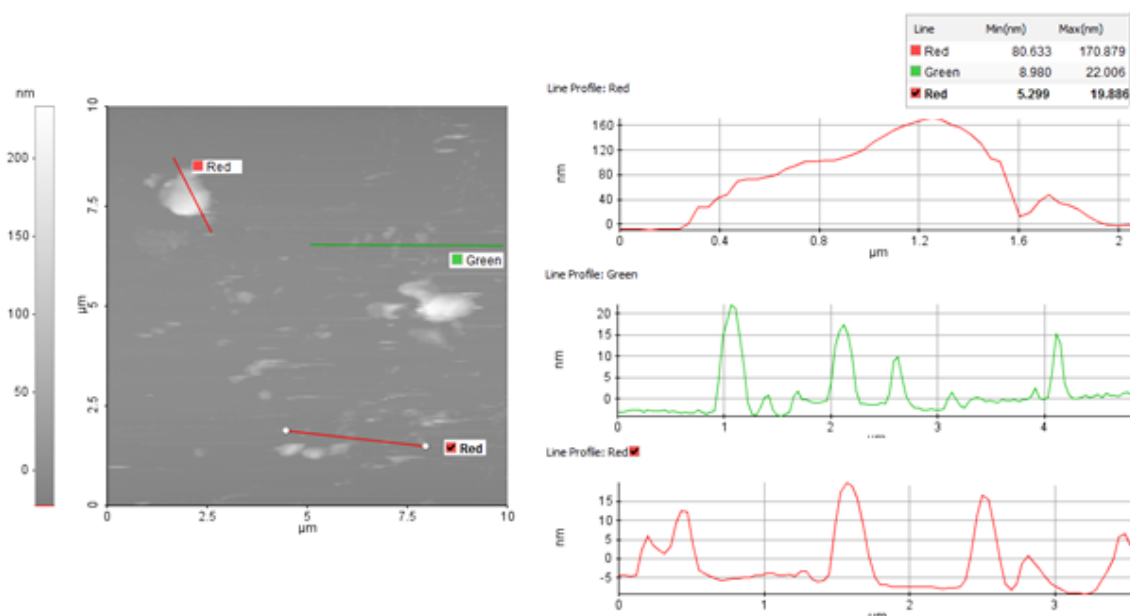
Figure 15 AFM image and cross-sectional height of leached particles for larger particle (red line) and smaller particles below 20 nm (red and green line) probably represent the elemental sulfur
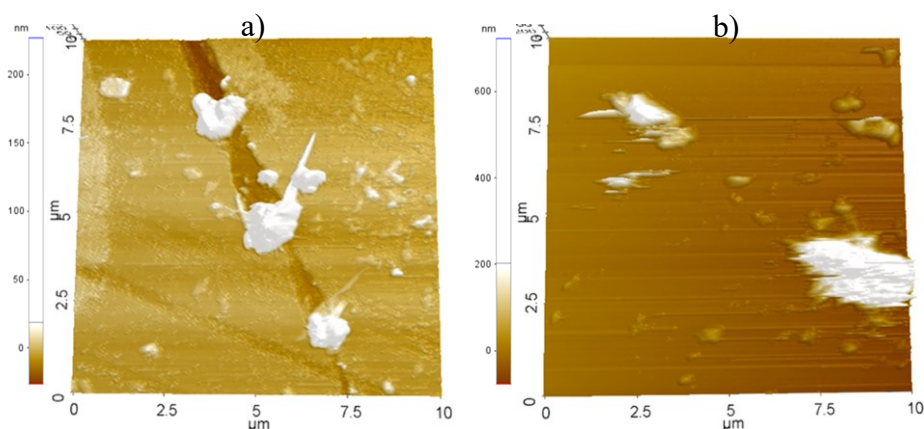
Figure 16 The comparison of precipitated iron (a) roast-leach process, (b) individual leach process

Figure 18 presents Zn-hydroxide precipitate that was in the form of rods as seen from the SEM image. Zn-hydroxide precipitate was then subjected to heat treatment in order to produce ZnO. According to XRD diffractions, ZnO phase in a good agreement with synthetic zincite was in spherical form as seen from the SEM and AFM in Figures 19 and 20, respectively. Similar SEM images were also found in the study on transformation of zinc hydroxide sulphate to crystalline zinc oxide [36].

Figure 21 also shows the line sectional height profiles of ZnO powders. Synthesized sub-micron ZnO particles could control the morphology, i.e., rings, bowls, hemispheres, and disks, depending on the reaction temperature, pH, and concentration of additive such as ammonium hydroxide. Moreover, it is known as agglomerated ZnO nanoparticles with a zincite structure having lack of defined shape and size [4, 37, 38, 39]. In the study on production of ZnO from zinc hydroxide carbonate by Moezzi et al (2014) [40], SEM images of the zinc hydroxide carbonate and the highly porous ZnO produced also showed that ZnO product was pseudomorphous with the hydrozincite precursor, as previously reported [41, 42].
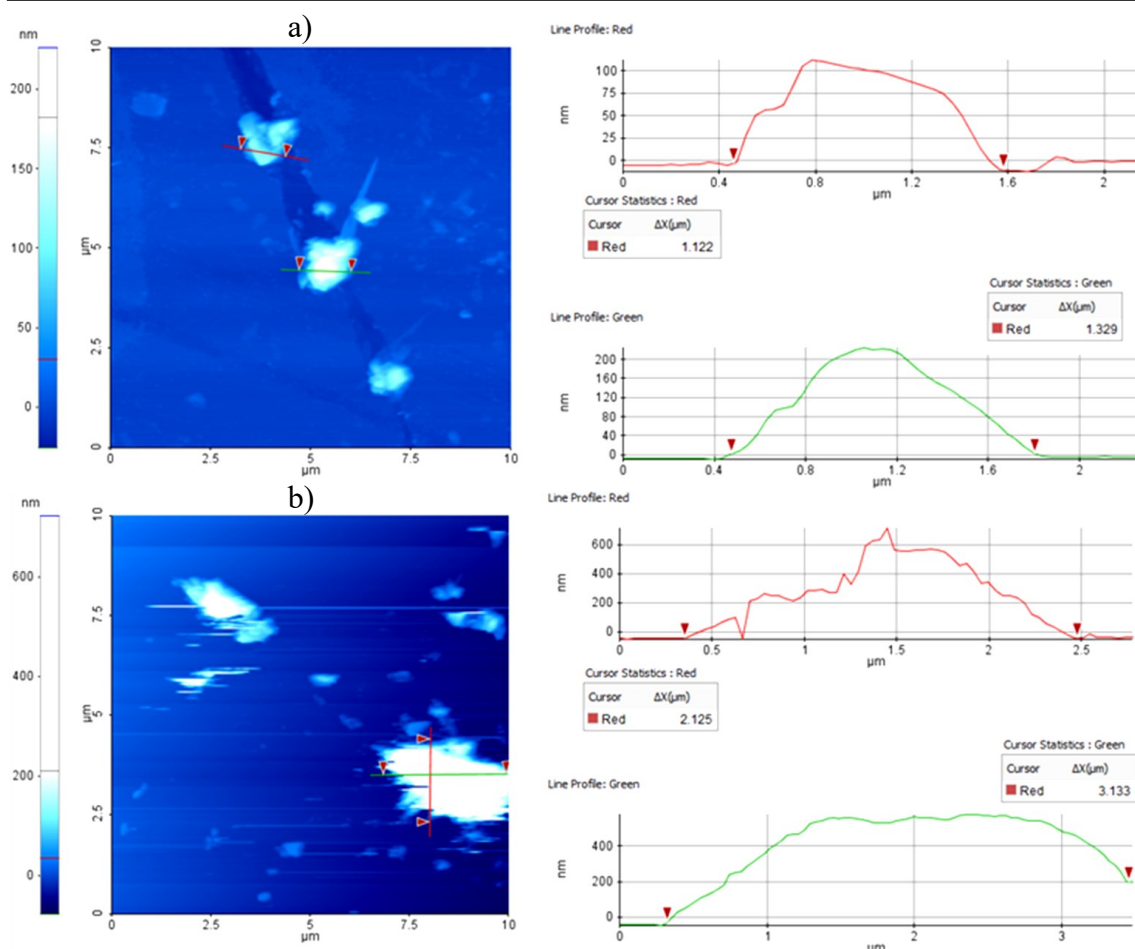
Figure 17 AFM image and cross-sectional height of precipitated Fe particles after (a) roast-leach process, (b) leach process

Figure 20 observed different shapes of the precipitated ZnO powders on a fresh mica disk as a result of the used preparation route. However, Figure 21 clearly shows the size range of precipitated ZnO nanoparticles on a mica disk. ZnO nanoparticles were counted under 20 nm in size and their averaged particle sizes were measured nearly 13 nm from the AFM image and its image analysis similar to the literature findings [40]. In that study, TEM images revealed that the ZnO pseudomorphous product is actually a polycrystalline aggregate comprised of individual crystals with sizes in the range of 5 to 20 nm and amorphous material was also detected [40]. However, in the study on transformation zinc hydroxide sulphate to crystalline zinc oxide, according to SEM studies, highly crystalline ZnO particles are observed, with grain sizes in the range of 100 to 500

nm [36]. Therefore, it is recommended that the further studies should be conducted on that part.
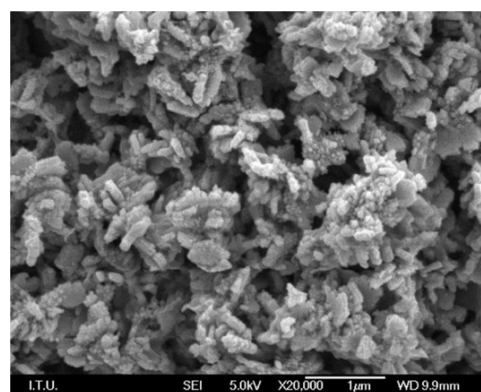
Figure 18 SEM photograph of zinc hydroxide precipitate
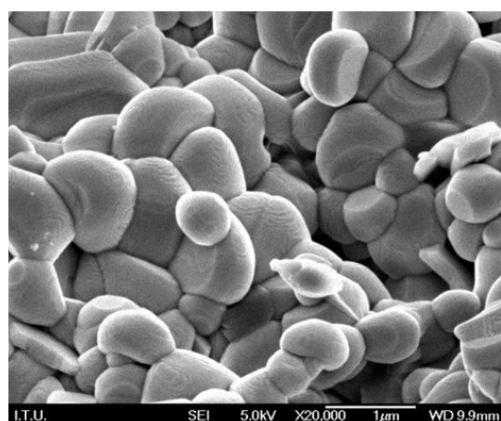
Figure 19 SEM image of ZnO clusters prepared from the zinc hydroxide
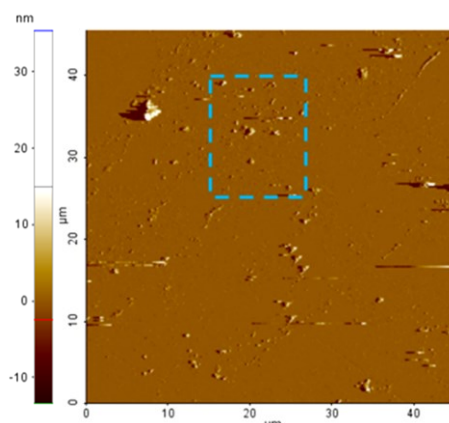
Figure 20 AFM image over 45x45 µm^2 regions of the precipitated ZnO nanopowders on a fresh mica prepared from Pb-Zn flotation tailings
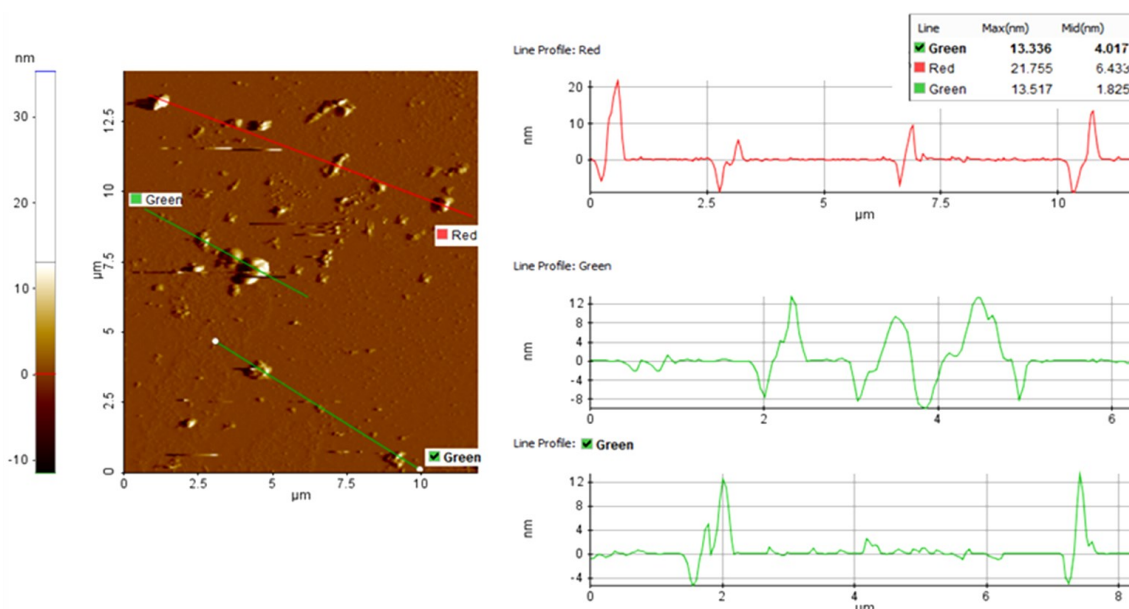
Figure 21 AFM image and cross-sectional heights of ZnO nanoparticles over 12.5x15 µm^2 regions (blue dashed in Fig. 18)

4.   Conclusion

The following conclusions were made as a result of this experimental study carried on lead-zinc flotation tailing:

1) Zinc oxide from the flotation tailings of mixed oxide-sulfide lead-zinc ore was successfully recovered by direct hydrometallurgical route and heat treatment when Zn dissolution efficiency was considered. 83.1% Zn and 91.6% Cd leaching efficiencies were obtained at the optimum conditions (20 g/L acid concentration, 1/5 S/L ratio, 1 hour leaching time, and 400 rpm stirring speed) while lead and iron were not dissolved in H_2SO_4 and the acid consumption was about 442.9 kg/t tailings.

2) Atomic force microscopy (AFM) image of the Pb-Zn flotation tailings before leaching clearly showed that the particles were in the sizes range of 50-110 nm. During the leaching in sulphuric acid solutions, majority of the particles was determined to be less than 20 microns according to the AFM image analysis.

3) Elemental sulfur started to form during direct acid leaching and produced a layer around the particles which was also revealed with SEM and AFM images. Leached particles were also identified a partially agglomerated particle in size of 170 nm.

4) Selective precipitations of iron and zinc in the form of hydroxide were performed with high recovery efficiencies of 90.1% and 99%, respectively. Zn-hydroxide precipitate was in the form of rods according to the SEM photo. After the heat treatment, synthetic zincite structures were produced in the mineral form of ZnO revealed by its XRD pattern with no impurity of Zn and $Zn(OH)_2$. The purity of spherical ZnO was found at 96.6%.

5) Nanocrystalline ZnO nanoparticles were also imaged from the AFM image and the nanoparticle image heights were measured less than 20 nm ZnO nanoparticles with a mean lateral diameter nearly 13 nm. Therefore, the flotation tailings ore can be a good recycling candidate for the production of high technology needs for nanocrystalline ZnO nanoparticles.

5. References

[1] Singh, S.C., Singh, D.P., Singh, J., Dubey, P.K., Tiwari, R.S., Srivastava, O.N. (2010) Metal Oxide Nanostructures; Synthesis, Characterizations and Applications. In: Umar, A. (Ed.) Encyclopedia of Semiconductor Nanotechnology, American Scientific Publishers.

[2] Ristic, M., Music, S., Ivanda, M., Popovic, S. (2005) Sol–gel synthesis and characterization of nanocrystalline ZnO powders. J. Alloys Compd., 397, L1-L4.

[3] Brayner, R., Dahoumane, S.A, Claude Yéprémian, C., Djediat, C., Meyer, M., Alain Couté, A., Fiévet, F. (2010) ZnO nanoparticles: synthesis, characterization, and ecotoxicological studies. Langmuir, 26, 6522- 6528.

[4] Vaseem, M., Umar, A., Hahn, Y.B. (2010) ZnO Nanoparticles: Growth, Properties, and Applications. In: Umar, A., Hahn, Y.B. (Eds.), Metal Oxide Nanostructures and Their Applications. American Scientific Publishers, Chapter 4, Volume 5, pp. 1-36.

[5] Hyk, W., Kitka, K., Rudnicki, D. (2019) Selective Recovery of Zinc from Metallurgical Waste Materials from Processing Zinc and Lead Ores. Molecules, 24, 2275, pp: 1-10.

[6] Zainuddin, N.A., Raja Mamat, T.A., Imam Maarof, H., Puasa, S.W., Mohd Yatim, S.R. (2019) Removal of Nickel, Zinc and Copper from Plating Process Industrial Raw Effluent Via Hydroxide Precipitation Versus Sulphide Precipitation, Joint Conference on Green Engineering Technology & Applied Computing 2019, IOP Conf. Series: Materials Science and Engineering 551 (2019) 012122, IOP Publishing.

[7] Caproni, G., Ciccu, R., Ghiani, M., Trudu, I. (1979) The Processing of Oxidized Lead and Zinc Ores in The Campo Pisano and San Giovanni Plants (Sardinia), XIII International Mineral Processing Congress, Processing of Oxidized and Mixed Oxide-Sulphide Lead-Zinc Ores, Warszawa, pp.71-91.

[8] Hosseini, S.H., Forssberg, K.S.E. (2002) Flotation of Oxidized Lead & Zinc Minerals from Angooran Deposit in Zanjan Province, Iran. IX International Mineral Processing Symposium, Extended Abstracts, 18-20 September, Cappadocia, Turkey, pp.105-106.

[9] Önal, G., Abramov, A.A. (2002) Optimal Conditions for Oxide Lead Minerals Flotation, IX International Mineral Processing Symposium, Extended Abstracts, 18-20 September 2002, Cappadocia, Turkey, 107-108.

[10] Onal, G., Bulut, G., Gül, A., Kangal, O., Perek, P.T., Arslan, F. (2005) Flotation of Aladag oxide lead–zinc ores. Miner. Eng. 18, 279-282.

[11] Perek, T., Benli, B., Arslan, F. (2011) Recovery of zinc from lead-zinc flotation tailings by leaching and precipitation. XIV International Balkan Mineral Processing Congress, June 14-16, Tuzla, Bosnia and Herzegovina.

[12] Buban, K.R., Collins, M.J., Masters, I.M. (1999) Iron control in zinc pressure leach processes, JOM, 51, 23-25.

[13] Principe, F.T., Demopoulos, G.P. (1999) The separation and concentration of iron from zinc process solutions. JOM, 51, 34-35.

[14] Ismael, M.R.C., Carvalho, J.M.R. (2003) Iron recovery from sulphate leach liquors in zinc hydrometallurgy. Minerals Engineering. 16, 31-39.

[15] Orhan, G. (2005) Leaching and Cementation of Heavy Metals from Electric Arc Furnace Dusts, Hydrometallurgy. 78, 236-245.

[16] Jitianu, M., Goia, D.V. (2007) Zinc oxide colloids with controlled size, shape, and structure. Journal of Colloid and Interface Science. 309, 78-85.

[17] Arslan, F., Aykaç, Y., Perek, K.T., Bakan, S., Önal, G. (2004) Leaching of Lead-Zinc Flotation Tailings, Proceedings of Xth International Mineral Processing

Symposium (Challenges and Opportunities in Mineral Processing), Çeşme-Turkey, pp. 667-671.

[18] Arslan, F., Aykaç, Y., Perek, K.T., Bakan, S., Önal, G. (2006) Evaluation of Lead-Zinc Flotation Tailings, in: Kongoli, F., Reddy, R.G. (Eds.), Sohn International Symposium on Advanced Processing of Metals and Materials: Thermo and physicochemical principles: special materials, aqueous and electrochemical processing, Volume 3, San Diego, USA, pp.387-395.

[19] Rahman, M.M., Qadir, M.R., Neger, A.T., Kurny, A.S.W. (2013) Studies on the Preparation of Zinc Oxide from Galvanizing Plant Waste. American Journal of Materials Engineering and Technology. 1, 4, 59-64.

[20] Ruiz, O., Clemente, C., Alonso, M., Alguacil, F.J. (2007) Recycling of an electric arc furnace flue dust to obtain high grade ZnO. J Hazard Mater., 141 (1), 33-6.

[21] Tsakiridis, P.E., Oustadakis, P., Katsiapi, A., Agatzini-Leonardou, A. (2010) Hydrometallurgical process for zinc recovery from electric arc furnace dust (EAFD). Part II: Downstream processing and zinc recovery by electrowinning. Journal of Hazardous Materials, 179, 8-14.

[22] Kunicky, Z., Jandova, J., Dostal, J., Dvorak, P. (2008) Zinc Recovery From Wastes Using Spent Acid From Scrapped Lead Acid Batteries. International Symposium on Lead and Zinc Processing, The Southern African Institute of Mining and Metallurgy, Republic of South Africa, pp. 247-254.

[23] Solookinejad Gh., Rozatian A.S.H., Habibi M.H. (2016) Zinc Oxide Thin Films Characterization, AFM, XRD and X-ray Reflectivity, Experimental Techniques (2016) 40: 1297-1306, Society for Experimental Mechanics.

[24] Benli, B. (2014) Effects of humic acid release from sepiolite on the interfacial and rheological properties of alkaline dispersions, Applied Clay Science, 102, 12/2014, 1-7.

[25] Plaschke, M., Schafer, T., Bundschuh., T., Manh, T.N., Knopp, R., Geckeis, H., Kim, J.I. (2001) Size characterization of bentonite colloids by different methods. Anal. Chem., 73, 4338-4347.

[26] Bickmore, B.R., Hochella, M.F., Bosbach, D., Charlet, L. (1999) Methods for performing atomic force microscopy imaging of clay minerals in aqueous solutions. Clays Clay Miner., 47, 573-581.

[27] Doutt D.R., Brillson L.J. (2011) Nanoscale AFM and KPFM Mapping of Localized Charge and Recombination Centers on Chemically active ZnO Surfaces, Case Study: ZnO Surfaces, Park System Applications Note, 1-5.

[28] Maroufa, S., Beniaichea, A., Guessasa, H., Azizib, A. (2017) Morphological, Structural and Optical Properties of ZnO Thin Films Deposited by Dip Coating Method, Materials Research, 20(1): 88-95.

[29] Katı, N. (2019) Investigation of Optical and Morphological Properties of Co Doped ZnO Nanomaterials, Turkish Journal of Science & Technology, 14(1), 41-48.

[30] Pourbaix, M. (1974) Atlas of Electrochemical Equilibria in Aqueous Solutions, Second English Edition, NACE (National Association of Corrosion Engineers) Houston, Texas, International Cebelcor.

[31] Perek, K.T., Arslan, F. (2003) Recovery of Metallic Values from Küre Massive Rich Copper Ores by Pressure Leaching, Istanbul Technical University Journal/d-Engineering, 2 (3), 65-72.

[32] Yoshida, T. (2003) Leaching of Zinc Oxide in Acidic Solution, Materials Transactions, Vol. 44, No. 12, pp. 2489-2493.

[33] Kim, Y., Lee, J. (2016) Leaching Kinetics of Zinc from Metal Oxide Varistors (MOVs) with Sulfuric Acid, Metals, 6, 192.

[34] Arslan, F., Bulut, G., Kangal, M.O., Perek, K.T., Gül, A., Gürmen, S. (2004) Studies on Leaching of Massive Rich Copper Ore Acidic Ferric Sulfate Solution, Scandinavian Journal of Metallurgy, 33 (1), 6-14.

[35] Cobble, J.R., Jordan, C.E., Rice, D.A. (2003) US Bureau of Mines RI 9472.

[36] Moezzi, A., Cortie, M.B., McDonagh, A.M. (2013) Zinc hydroxide sulphate and its transformation to crystalline zinc oxide, Dalton transactions, Issue 42, 14432-14437.

[37] Lee, B.W., Koo, J.H., Lee, T.S., Kim, Y.H., Hwang, J.S. (2013) Synthesis of ZnO Nanoparticles via Simple Wet-Chemical Routes, Advanced Materials Research, Vol. 699, pp 133-137.

[38] John, M., Heuss-Aßbichler, S., Ullrich, A. (2016) Recovery of Zn from wastewater of zinc plating industry by precipitation of doped ZnO nanoparticles, Int. J. Environ. Sci. Technol. (2016) 13:2127–2134.

[39] Shamhari, N.M., Wee, B.S., Chin, S.F., Kok, K.Y. (2018) Synthesis and Characterization of Zinc Oxide

Nanoparticles with Small Particle Size Distribution, Acta Chim. Slov. 65, 578–585.

[40] Moezzi, A., Cortie, M., Dowd, A., McDonagh, A. (2014) On the Formation of Nanocrystalline Active Zinc Oxide from Zinc Hydroxide Carbonate, Journal of Nanoparticle Research, 16, Article Number: 2344.

[41] Castellano, M., Matijevic, E. (1989) Uniform colloidal zinc compounds of various morphologies, Chemistry of Materials, 1:78-82.

[42] Kanari, N., Mishra, D., Gaballah, I., Dupré, B. (2004) Thermal decomposition of zinc carbonate hydroxide, Thermochimica Acta 410:93-100.

[43] Jandová, J., Dvorák, P., Jiričný, V., Mráz, R. (2003) Recycling of ZnO Flue Dust to Produce Zinc by Hydrometallurgical Routes, in: Young, C., Alfantazi, A., Anderson, C., James, A., Dreisinger, D., Harris, B. (Eds.), Electrometallurgy and Environmental Hydrometallurgy, John Wiley & Sons, Inc., Hoboken, NJ, Volume 2, pp.1509-1603.

DOBIJANJE ZnO IZ FLOTACIJSKE JALOVINE KOJA SADRŽI OLOVO I CINK HIDROMETALURŠKIM POSTUPCIMA – XRD, SEM I AFM ANALIZE

K.T. Perek[1], B. Benli[1], C. Arslan[2], F. Arslan[1#]

[1]Istanbul Technical University, Mineral Processing Engineering Department, Istanbul, Turkey
[2]Istanbul Technical University, Metallurgical and Material Engineering Department, Istanbul, Turkey

Izvod

Hidrometalurška metoda za dobijanje cink hidroksida i sintezu ZnO nanokristalne strukture predstavlja veoma interesantnu metodu za dobijanje oksida olova i cinka iz flotacijske jalovine koja sadrži olovo i cink. U Turskoj, rude koje pored olova i cinka imaju i visoki sadržaj gvožđa nisu pogodne za uobičajene metode koje se koriste za preradu mineralnih sirovina i potrebno je koristiti hidrometalurške metode. Stoga, kontrola gvožđa tokom postupaka koji uključuju cink je veoma važna. U ovom radu je ispitivana hidrometalurška metoda za dobijanje cinka iz Pb-Zn flotacijske jalovine tako što je ispitivan uticaj koncentracije H_2SO_4 i temperature prilikom luženja i prženja na rastvaranje cinka uzimajući u obzir promenu redoks-potencijala i pH vrednosti. Dobijeni uzorci gvožđa i cinka su pojedinačno analizirani metodama rentgenske difrakcije (XRD), pretražnog elektronskog mikroskopa (SEM) i mikroskopa atomskih sila (MAS) (engl. Atomic Force Microscope, AFM) da bi se uporedili uzorci pre i posle luženja, taloženja i prženja. Dobijeno je 83,1% Zn i 91,6% Cd postupkom luženja iz Pb-Zn flotacijske jalovine, gde su veličine čestica bile od 50 do 110 nm što se vidi na presecima slika dobijenih mikroskopijom atomskih sila, dok se olovo i gvožđe nisu rastvorili. Elementarni sumpor je počeo da se formira i stvara sloj oko čestica ili delimično nagomilanih čestica veličine 170 nm tokom postupka luženja u prisustvu sumporne kiseline. Međutim, utvrđeno je da je veličina većine čestica bila manja od 20 mikrona, a slike dobijene mikroskopom atomskih sila su pokazale da se veličina luženih i neluženih čestica razlikovala za više od 50%.

Selektivno taloženje gvožđa i cink hidroksida je postignuto u velikom procentu, 90,1% gvožđa i 99% cinka. Nakon termičkog postupka, dobijeni su klasteri cinka čistoće 96,6% u obliku minerala ZnO i veličine skoro 13 nm. Dobijanje cinka se može smatrati uspešnim, a flotacijska jalovina se može posmatrati kao dobar kandidat za proizvodnju visokotehnoloških nanočestica ZnO sa nanokristalnom strukturom.

Ključne reči: *Pb-Zn rude; Luženje; Taloženje; Klasteri cink oksida; Struktura cink-oksida.*